ACS Catalysis

pubs.acs.org/acscatalysis Letter

Unveiling the Synthetic Potential of Substituted Phenols as Fully Recyclable Organophotoredox Catalysts for the Iodosulfonylation of Olefins

Cristian Rosso,[⊥] Sara Cuadros,[⊥] Giorgia Barison, Paolo Costa, Marina Kurbasic, Marcella Bonchio, Maurizio Prato, Luca Dell'Amico,* and Giacomo Filippini*

Cite This: *ACS Catal.* 2022, 12, 4290−4295 Read Online

ACCESS | Metrics & More | Article Recommendations | Supporting Information

ABSTRACT: We describe an efficient photocatalytic procedure for the direct iodosulfonylation of terminal olefins **3** with α-iodo phenylsulfones **4**. Specifically, the process uses the simple, robust, and fully recyclable phenol derivative **6e** as the precatalytic system and occurs with visible-light irradiation (450 nm). Mechanistic investigations proved the key role of the *in situ* generated photocatalyst, namely phenolate anion **7e**, which has shown high catalytic activity and considerable stability toward the operating conditions. Importantly, this photocatalytic transformation provides a wide variety of densely functionalized alkyl iodides **5** (23 examples, up to 95% yield). Finally, the synthetic potential of this photochemical transformation was demonstrated by scaling up the process under microfluidic conditions (up to 0.67 mmol h^{-1}) while accessing a series of relevant product manipulations.

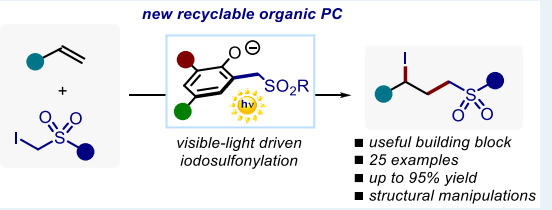

KEYWORDS: *photoredox catalysis, organic photocatalyst, organocatalysis, iodosulfonylation, olefin transformation*

Over the past decade, the field of photocatalysis has experienced a tremendous growth.[1] Photocatalysis allows unique reactivity pathways that are impossible to access under classical thermal protocols.[2] In particular, photoredox catalysis, which involves the light-triggered movement of one electron from or to an organic substrate, has been established as a key enabling technology for the mild functionalization of organic molecules.[3] However, many of the most commonly employed visible-light photoredox catalysts (PCs) are polypyridyl complexes of ruthenium or iridium,[3a] which are expensive and often environmentally harmful. For this reason, extensive effort is still focusing on the development of more sustainable metal-free photocatalyzed transformations.[1a,4] Specifically, the synthetic community is moving toward the use of purely organic PCs, which are cheaper and more sustainable options with respect to metal complexes, while allowing an easy fine tuning of their optoelectronic properties.[1a,5] In this context, phenolate anions, generated upon the deprotonation of phenols or suitable cyclic ketones, are electron-rich aromatic intermediates capable of promoting visible-light-driven transformations.[6] Interestingly, upon light absorption phenolates become strong reductants in the excited state capable of triggering the generation of radicals from diverse precursors via single-electron-transfer (SET) processes.[7] Nevertheless, phenolate anions often turn out to be highly unstable in the presence of reactive radicals. In fact, these species can efficiently react with open-shell radicals through homolytic aromatic substitution (HAS) pathways or undergo side reactions such as radical polymerization processes, thus hampering their use under catalytic regimes.[6a,8] To overcome this limitation, a careful design of the chemical structure of the phenolate anion is pivotal to finely tune its optical and redox properties, thus imparting a higher stability and efficiency to the resulting PCs. As a matter of fact, only few photocatalytic protocols fulfilling these features have been reported so far.[6b,9] In 2019, König and co-workers reported that a tricyclic aromatic ketone, namely 9-anthrone (**1**), can act as an effective pre-PC.[9b] Indeed, **1** can be easily deprotonated under basic conditions, producing a a photoactive phenolate anion that was used to catalyze C−H arylation reactions between aryl halides and electron-rich arenes and heteroarenes under visible-light irradiation (Figure 1a).

Later on, the same research group demonstrated that anthrone derivatives may also be employed as robust pre-PCs to promote the photochemical carboxylation of organic compounds with CO_2.[9d] In 2020, Xia and co-workers described a new photocatalytic protocol for the direct oxyarylation reaction of olefins with aryl halides and 2,2,6,6-tetramethylpiperidin-1-ol (TEMPO-H, Figure 1b).[9c] Specifically, the authors found that a trisubstituted phenolate anion,

Received: February 1, 2022
Revised: March 21, 2022
Published: March 25, 2022

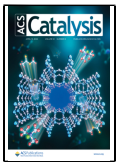

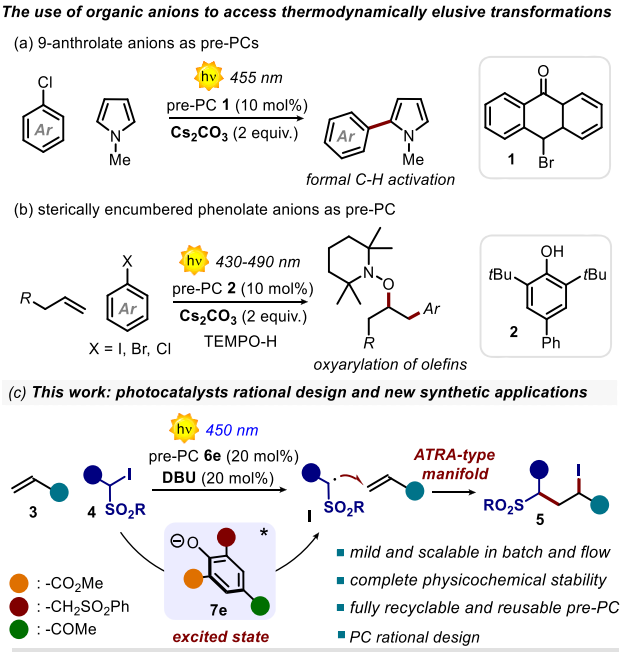

Figure 1. (a) Use of 9-anthrone (**1**) in the photocatalytic C−H arylation of electron-rich arenes.[9b] (b) Photocatalytic oxyarylation of olefins with aryl halides and TEMPO-H.[9c] (c) This work: light excitation of a 2,4,6-trisubstituted phenolate (**7e**) enabling the direct iodosulfonylation of olefins (**3**) with α-iodo phenylsulfones (**4**). DBU: 1,8-diazabicyclo[5.4.0]undec-7-ene.

formed upon deprotonation of **2** (pre-PC) with Cs_2CO_3, displayed the best synthetic performance.

Herein, we document the design and structural refinement of a novel efficient organic PC based on a 2,4,6-trisubstituted phenolate scaffold (**7e**, Figure 1c). The PC's structural design was guided by the goal of developing an unprecedented photocatalytic atom transfer radical addition (ATRA) process between α-iodo phenylsulfones (**4**) and terminal olefins (**3**) to produce synthetically valuable sulfone-containing alkyl halides (**5**) in a single strike.[10] Remarkably, the process was efficiently orchestrated by the photochemical activity of the 2,4,6-trisubstituted phenolate **7e**, easily formed *in situ* by deprotonating the corresponding phenol **6e** (pre-PC) with 1,8-diazabicyclo[5.4.0]undec-7-ene (DBU). Thanks to the high chemical stability and photocatalytic efficiency of the newly developed PC, we were able to access a mild and general iodosulfonylation process under batch and flow (up to 0.67 mmol h^{-1}) conditions, while recovering and reusing the PC up to six consecutive times without any drop in yield. To the best of our knowledge, this is the first example of photocatalysis with a fully recyclable phenol-based PC.

We initiated our study evaluating diverse readily available phenols **6** as pre-PCs (20 mol %) for the reaction between olefin **3a** and the α-iodosulfone **4a** (Table 1a and SI).

The experiments were conducted at ambient temperature under irradiation at 450 nm over 24 h, using acetonitrile as the solvent and in the presence of DBU (20 mol %) as the base. Quite surprisingly, the simple phenol **6a** ($\lambda_{0,0}$(**7a**) = 277 nm) delivered the desired product **5a** in a promising yield (47%). However, most of **6a** was converted into a complex mixture of degradation products under the reaction conditions. We next sought to evaluate the activity of 2-bromophenol (**6b**), which has similar redox properties (see Table 1a).[9a] Regrettably, **6b**

Table 1. Optimization of the Photocatalytic ATRA Process and Control Experiments—Selected Results

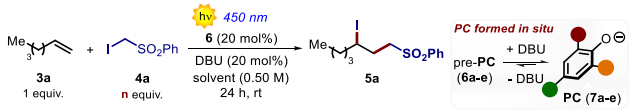

(a) phenolate PC screening

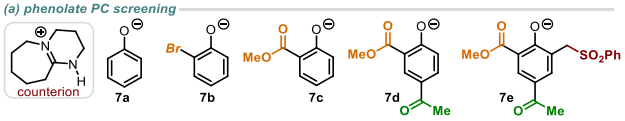

	7a	7b	7c	7d	7e
$\lambda_{0,0}$	277 nm	258 nm	312 nm	372 nm	***378 nm***
$E_{0,0}$	4.48 V	4.81 V	3.97 V	3.33 V	***3.28 V***
E_{ox}	+ 0.30 V	+ 0.34 V	+ 0.50 V	+ 0.65 V	***+ 0.74 V***
E^*_{ox}	- 4.18 V	- 4.47 V	- 3.47 V	- 2.68 V	***- 2.54 V***
yield (5a)[b]	47%	56%	52%	53%	***85%***
residual (6)[b]	35%	87%	<5%	85%	***>99%***

(b) optimization of the reaction conditions

entry[a]	4a (equiv.)	solvent	additives and conditions	yield % (5a)[b]	residual % (6)[b]
1	1.0	MeCN	-	85%	>99%
2	1.5	MeCN/H_2O (3:1)	NaAsc (25 mol%)	>99%	>99%
3	1.5	MeCN/H_2O (3:1)	NaAsc (25 mol%) *in the dark or at 525 nm*	0%	>99%
4	1.5	MeCN/H_2O (3:1)	NaAsc (25 mol%) *without* **6e** *and* DBU	8%	>99%
5	***1.5***	***MeCN/H_2O (3:1)***	***NaAsc (25 mol%) 8 h***	***>99%***	***>99%***

[a]Reactions performed on a 0.2 mmol scale using 0.04 mmol of phenol **6**. [b]The yield and residual phenol (**6**) were determined by ^{1}H NMR analysis of the crude reaction product, using trichloroethylene as internal standard. NaAsc: sodium ascorbate.

turned out to not be particularly effective with only a slight improvement (56% yield), although it had higher stability with respect to **6a** (87% recovery). Replacing the Br substituent with a methyl ester resulted in a strong bathochromic shift with the $\lambda_{0,0}$ value changing from 258 nm (**7b**) to 312 nm (**7c**), while a similar chemical yield was observed (52 %). However, in this case the pre-PC **6c** was largely converted into a mixture of alkylated products, derived from a side reaction with the *in situ* generated sulfonyl radical **I**. We thus reasoned that placing an additional electron-withdrawing group (EWG) at the *para* position would increase the chemical stability, rendering the PC **7d** less reactive toward the alkylation for both electronic and steric reasons. Indeed, the chemical stability of the pre-PC increased and **6d** was recovered in 85% yield, along with 12% of the *ortho*-alkylated side product **6e** (Table 1a). Nevertheless, the yield of **5a** was unchanged (53%). At this stage, we hypothesized using the byproduct **6e** as a pre-PC in the model transformation. We selected **6e** and the corresponding phenolate **7e**, since the presence of two EWGs with an additional sulfone moiety (i) resulted in a strong aromatic ability for absorption in the visible spectral region[11] and (ii) furnished higher stability of the PC to HAS, while (iii) presenting an altered distribution of the molecular orbitals with respect to all of the other phenolates. Density functional theory (DFT) calculations revealed that in **7e** the highest occupied molecular orbital (HOMO) is located on the aromatic core and the lowest unoccupied molecular orbital (LUMO) lies on the sulfone moiety (see the Supporting Information). The spatial separation of the HOMO and LUMO orbital implies that this PC is able to access a charge transfer (CT) excited state,[5b,12] as corroborated by the characteristic Stokes shift (see the Supporting Information) and the more balanced redox properties (E_{ox}(**7e**) = +0.74 V vs SCE, E^*_{ox}(**7e**) = −2.54 eV). Interestingly, the use of **6e** led to the formation of **5a** in

https://doi.org/10.1021/acscatal.2c00565
ACS Catal. 2022, 12, 4290−4295

excellent chemical yield (85%), which in turn was accompanied by a virtually complete chemical stability of its corresponding phenolate (**7e**, >99% residual pre-PC).

Further optimization (Table 1b and the Supporting Information) revealed that a slight excess of **4a** (1.5 equiv), a 3/1 mixture of MeCN and H_2O as solvent, and addition of 25 mol % of sodium ascorbate (NaAsc) led to the formation of **5a** in a quantitative yield (entry 2, Table 1b). The addition of NaAsc was key for allowing a more efficient *in situ* regeneration of the photoreactive phenolate **7e** (*vide infra*, Figure 2a).[13] A

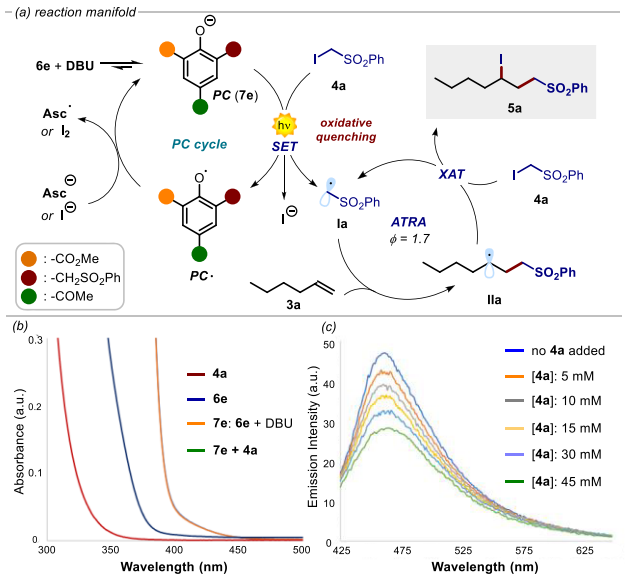

Figure 2. (a) Mechanism of the photocatalytic ATRA process. (b) Optical absorption spectra recorded in MeCN: [**4a**] = 0.005 M (red line); [**6e**] = 0.001 M (blue line); [DBU] = 0.001 M. The green line (**7e** + **4a**) overlaps with the orange line (**7e**). (c) Quenching of the phenolate **7e** emission ([**7e**] = 0.015 M in MeCN, excitation at 410 nm) in the presence of increasing amounts of **4a**.

control experiment confirmed the light-driven nature of the iodosulfonylation process (entry 3, Table 1b). In addition, we demonstrated that the photochemical activity of the phenolate anion **7e** was essential for triggering the intended reactivity. Indeed, compound **5a** was obtained in very poor yield (8%), when the reaction was run in the absence of the photocatalytic system (entry 4, Table 1b). Finally, we were able to reduce the reaction time to 8 h, without any erosion in yield (entry 5, Table 1b). It is important to emphasize that other organic bases such as 1,5-diazabicyclonon-5-ene (DBN) and 1,1,3,3-tetramethylguanidine (TMG) can be efficiently employed in place of DBU under the reaction conditions, whereas basic organic and inorganic salts turned out to be ineffective (see section F of the Supporting Information).

It is worth noting that across all of the experiments (entries 1−5, Table 1b) we were able to quantitatively recover the pre-PC **6e**. This fact confirms our initial hypothesis that **7e** can produce open-shell species without taking part in the radical process. From a mechanistic point of view (Figure 2), the ATRA-type process begins with the *in situ* generation of the phenolate of **6e**, namely **7e**. Indeed, upon addition of DBU, the solution of **6e** (blue line in Figure 2b), which was almost colorless, immediately turned bright yellow, indicating the ability of the phenolate **7e** to absorb in the visible spectral region (orange line in Figure 2b). Addition of the iodide **4a** did not bring about any appreciable change of the absorption spectrum (green line in Figure 2b, perfect overlap with the absorption of **7e**), which excluded the formation of an electron-donor−electron-acceptor (EDA) complex with the phenolate **7e**.[14] This was further corroborated by performing a series of ^{1}H NMR spectroscopic studies in deuterated acetonitrile (see the Supporting Information), where the presence of **4a** did not induce any detectable shift of the proton signals of **7e** toward a higher ^{1}H NMR field.[15] Importantly, we have recorded the emission spectra of **7e** upon excitation at 410 nm (Figure 2c, maximum emission at 470 nm). A series of Stern−Volmer quenching studies were performed, which revealed that the radical precursor **4a** effectively quenched the excited state of **7e**. On the basis of these experimental observations, we propose that, upon light absorption, **7e** directly reaches an electronically excited state (**7e***) to become a strong reductant, as implied by its reduction potential, which was measured to be −2.54 V (vs SCE). This excited species effectively triggers the formation of the electron-deficient radical **Ia** through the reductive cleavage of the C−I bond in **4a** (E_{red} = −1.4 V vs SCE).[16] After the photochemical initiation step, the radical **Ia** enters a chain cycle. Here, the olefin **3a** intercepts **Ia**, generating **IIa** (Figure 2a). This radical intermediate undergoes halogen-atom transfer (XAT)[17] with **4a**, forming the final product **5a** and regenerating **Ia**. This scenario is congruent with the quantum yield (Φ) of 1.7 measured for the model reaction (see the Supporting Information), which confirms the activity of a radical chain process.[18] Interestingly, under the optimized reaction conditions, we did not observe the formation of any polymeric byproducts arising from the possible atom transfer radical polymerization (ATRP) of **3a**.[19] Using the optimized reaction conditions, we demonstrated the generality of the photocatalytic iodosulfonylation reaction with respect to the alkene component **3**. As shown in Figure 3, the reaction efficiently tolerates various terminal olefins bearing alkyl chains and alcohol, silyl ether, ether, ester, sulfone, imide, indole, ketone, and halide moieties (products **5a−n**). On the other hand, we successfully used other phenyl- and alkyl-substituted α-iodosulfones as radical precursors (products **5p−x**). In all of the cases we registered good to excellent yields (up to 95%). As limitations, styrene and α-iodobenzyl sulfone did not participate in the developed process (products **5o,y**). Similarly, 1,1- and 1,2-disubstituted alkenes did not lead to the formation of the corresponding ATRA-type products in satisfactory yields, probably due to their increased steric hindrance (see section G of the Supporting Information). We next evaluated a scaling-up of the photocatalytic ATRA process by using a microfluidic photoreactor (MFP).[1b,20] Gratifyingly, the reaction was readily implemented under flow conditions without the need for further optimization of the reaction conditions (Figure 4a). Nevertheless, the presence of sodium ascorbate (NaAsc) and water was not tolerated by the microfluidic apparatus, resulting in inferior yields with respect to the batch photoreactions (53% versus 82%), while allowing the isolation of 0.49 g of the product **5a** after only 3 h overall reaction time, with a residence time (t_R) as short as 5 min (productivity of 0.67 mmol h^{-1} vs 0.02 mmol h^{-1} for the batch procedure).

We decided to use this reaction, which involves the presence of diverse reactive radical intermediates to assess the chemical stability of the developed photocatalytic system **7e** and the recyclability of the pre-PC **6e**. We thus performed five iterative independent reactions, where **6e** was recovered at the end of

https://doi.org/10.1021/acscatal.2c00565
ACS Catal. 2022, 12, 4290−4295

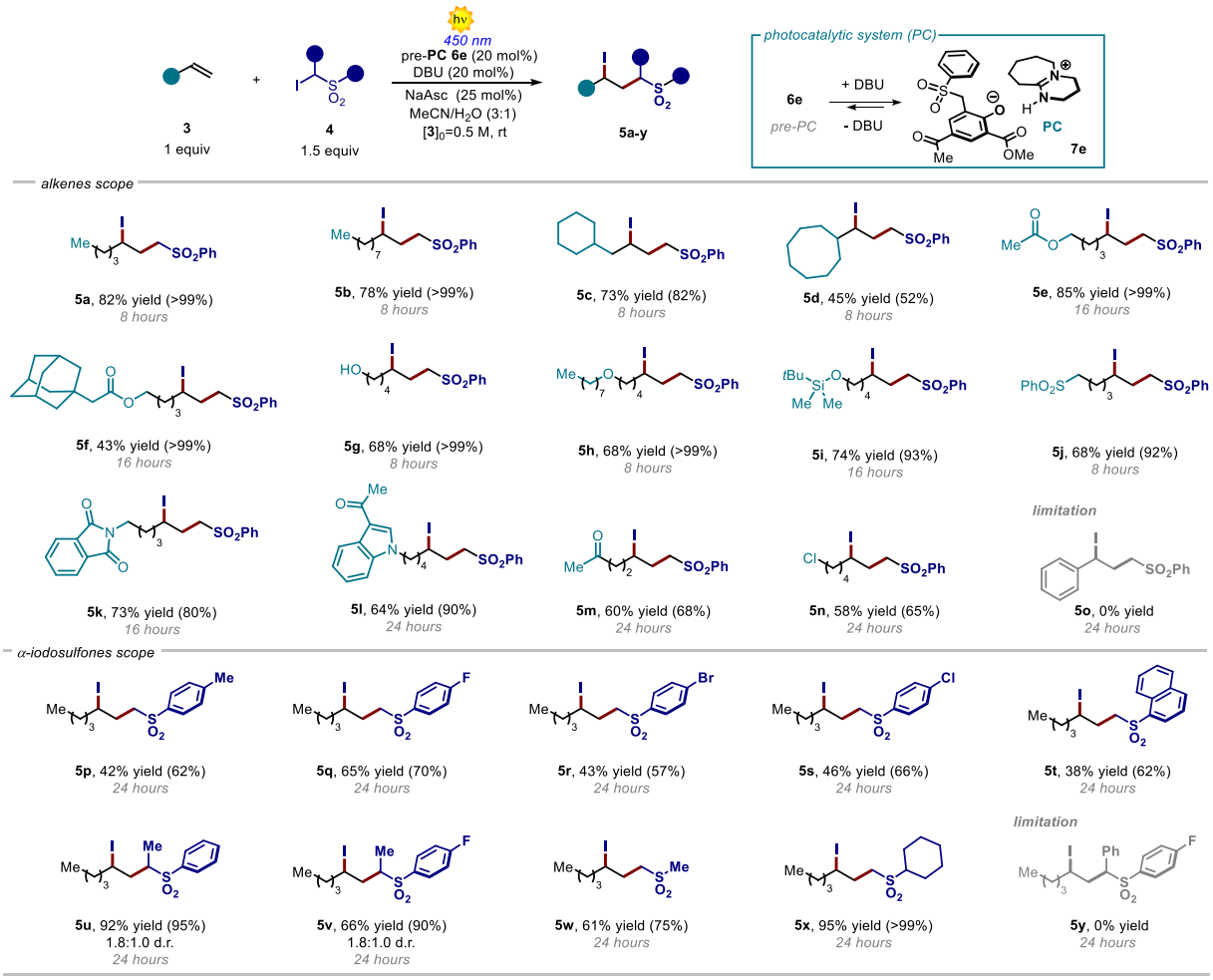

Figure 3. Scope of α-iodosulfones **4** and alkenes **3** that can participate in the ATRA process. Reactions were performed on a 0.2 mmol scale using 1.5 equiv of **4** under batch conditions. Yields in parentheses were determined by ^{1}H NMR analyses, using trichloroethylene as an internal standard.

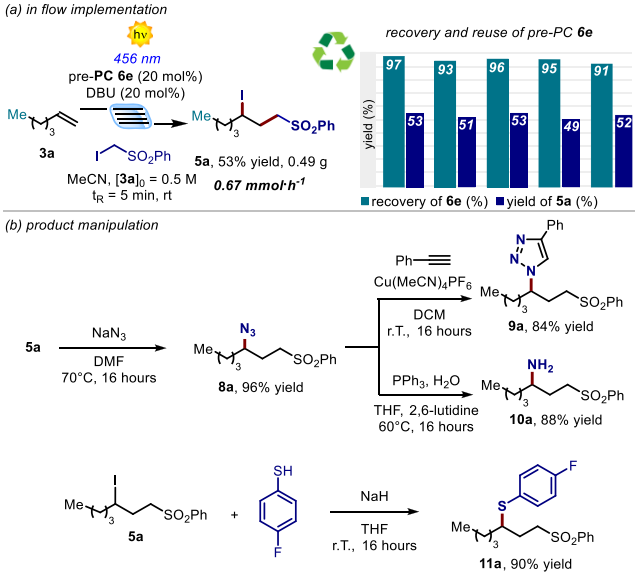

Figure 4. (a) Recyclability and performances of the pre-PC **6e** under flow conditions. (b) Manipulations of the ATRA product **5a**.

each run by extraction and filtration and reused in the following run. At every run, we evaluated the performance of the system by monitoring the yield of **5a**. Importantly, we were able to recover the pre-PC **6e** in almost quantitative yield (91−97%), indicating its excellent chemical robustness. Accordingly, the photocatalytic performance of the system was constant with yields spanning from 53% to 49%. This set of experiments confirms the potential of the developed phenol **6e** as a fully recyclable, purely organic pre-PC. In order to further demonstrate the synthetic potential of the developed photocatalytic iodosulfonylation process, we decided to carry out manipulation reactions (Figure 4b). The product **5a** was effectively transformed into the corresponding azide-containing derivative: namely, **8a**. The azide group was subsequently used to increase the molecular complexity, hence giving products **9a** and **10a** in excellent isolated yields (up to 88%), through a Cu-catalyzed click reaction and a Staudinger reduction, respectively. These results prove the high versatility of the building blocks **5**, while they demonstrate the synthetic relevance of the developed iodosulfonylation process. Finally, **5a** was also treated in the presence of 4-fluorothiophenol to obtain thioether **11a** in excellent isolated yield (90%), showing an additional structural motif that can be easily accessed by routine synthetic operations.

In conclusion, we have developed a new metal-free photocatalytic strategy that enables the direct iodosulfonylation of olefins **3** with α-iodo phenylsulfones **4**, under mild reaction conditions. In this reaction, the trisubstituted phenol

https://doi.org/10.1021/acscatal.2c00565
ACS Catal. 2022, 12, 4290−4295

6e acts as a robust and fully recyclable organic pre-PC that was easily recovered and reused up to five times without any significant drop in yield. Overall, these findings open new possibilities in olefin-directed functionalization methods, while establishing a new easy to make and recyclable organic photocatalytic system with the synthetic potentials demonstrated herein.

■ ASSOCIATED CONTENT

Supporting Information

The Supporting Information is available free of charge at https://pubs.acs.org/doi/10.1021/acscatal.2c00565.

Experimental procedures, characterization data, and UV and NMR spectra (PDF)

■ AUTHOR INFORMATION

Corresponding Authors

Luca Dell'Amico − *Department of Chemical Sciences, University of Padova, 35131 Padova, Italy;* orcid.org/0000-0003-0423-9628; Email: luca.dellamico@unipd.it

Giacomo Filippini − *Department of Chemical and Pharmaceutical Sciences, CENMAT, Center of Excellence for Nanostructured Materials, INSTM UdR, Trieste, University of Trieste, 34127 Trieste, Italy;* orcid.org/0000-0002-9694-3163; Email: gfilippini@units.it

Authors

Cristian Rosso − *Department of Chemical and Pharmaceutical Sciences, CENMAT, Center of Excellence for Nanostructured Materials, INSTM UdR, Trieste, University of Trieste, 34127 Trieste, Italy;* orcid.org/0000-0002-1254-0528

Sara Cuadros − *Department of Chemical Sciences, University of Padova, 35131 Padova, Italy*

Giorgia Barison − *Department of Chemical Sciences, University of Padova, 35131 Padova, Italy;* orcid.org/0000-0001-8125-3293

Paolo Costa − *Department of Chemical Sciences, University of Padova, 35131 Padova, Italy;* orcid.org/0000-0001-6324-1424

Marina Kurbasic − *Department of Chemical and Pharmaceutical Sciences, CENMAT, Center of Excellence for Nanostructured Materials, INSTM UdR, Trieste, University of Trieste, 34127 Trieste, Italy*

Marcella Bonchio − *Department of Chemical Sciences, INSTM UdR, Padova, University of Padova, 35131 Padova, Italy; Istituto per la Tecnologia delle Membrane, ITM-CNR, UoS di Padova, 35131 Padova, Italy;* orcid.org/0000-0002-7445-0296

Maurizio Prato − *Department of Chemical and Pharmaceutical Sciences, CENMAT, Center of Excellence for Nanostructured Materials, INSTM UdR, Trieste, University of Trieste, 34127 Trieste, Italy; Center for Cooperative Research in Biomaterials (CIC biomaGUNE), Basque Research and Technology Alliance (BRTA), 20014 Donostia San Sebastián, Spain; Basque Fdn Sci, Ikerbasque, 48013 Bilbao, Spain;* orcid.org/0000-0002-8869-8612

Complete contact information is available at: https://pubs.acs.org/10.1021/acscatal.2c00565

Author Contributions

[⊥]C.R. and S.C. contributed equally.

Funding

This work was supported by the University of Padova P-DiSC#11BIRD2020-UNIPD (L.D.), the CariParo Foundation, Synergy−Progetti di Eccellenza 2018 (L.D.), and the MIUR (PRIN Nanoredox, Prot. 2017PBXPN4; M.P., M.B.). G.F. kindly acknowledges FRA2021 funded by the University of Trieste and Microgrants 2021 funded by Region FVG (LR 2/2011, ART. 4). Part of this work was performed under the Maria de Maeztu Units of Excellence Program from the Spanish State Research Agency, Grant No. MDM-2017−0720.

Notes

The authors declare no competing financial interest.

■ ACKNOWLEDGMENTS

P.C. acknowledges the Seal of Excellence@UNIPD, Quanta-COF, for a postdoctoral fellowship. Prof. Paolo Melchiorre is acknowledged for fruitful discussions.

■ REFERENCES

(1) (a) Romero, N. A.; Nicewicz, D. A. Organic Photoredox Catalysis. *Chem. Rev.* **2016**, *116*, 10075−10166. (b) Buglioni, L.; Raymenants, F.; Slattery, A.; Zondag, S. D. A.; Noël, T. Technological Innovations in Photochemistry for Organic Synthesis: Flow Chemistry, High-Throughput Experimentation, Scale-up, and Photoelectrochemistry. *Chem. Rev.* **2022**, *122*, 2752−2906.

(2) Marzo, L.; Pagire, S. K.; Reiser, O.; König, B. Visible-Light Photocatalysis: Does It Make a Difference in Organic Synthesis? *Angew. Chem., Int. Ed.* **2018**, *57*, 10034−10072.

(3) (a) Shaw, M. H.; Twilton, J.; MacMillan, D. W. C. Photoredox Catalysis in Organic Chemistry. *J. Org. Chem.* **2016**, *81*, 6898−6926. (b) Twilton, J.; Le, C. C.; Zhang, P.; Shaw, M. H.; Evans, R. W.; MacMillan, D. W. C. The Merger of Transition Metal and Photocatalysis. *Nat. Rev. Chem.* **2017**, *1*, 0052.

(4) (a) Nicewicz, D. A.; Nguyen, T. M. Recent Applications of Organic Dyes as Photoredox Catalysts in Organic Synthesis. *ACS Catal.* **2014**, *4*, 355−360. (b) Bortolato, T.; Cuadros, S.; Simionato, G.; Dell'Amico, L. The Advent and Development of Organophotoredox Catalysis. *Chem. Commun.* **2022**, *58*, 1263−1283. (c) Rosso, C.; Filippini, G.; Prato, M. Use of Perylene Diimides in Synthetic Photochemistry. *Eur. J. Org. Chem.* **2021**, *2021*, 1193−1200.

(5) (a) Mateos, J.; Cuadros, S.; Vega-Peñaloza, A.; Dell'amico, L. Unlocking the Synthetic Potential of Light-Excited Aryl Ketones: Applications in Direct Photochemistry and Photoredox Catalysis. *Synlett* **2022**, *33*, 116−128. (b) Vega-Peñaloza, A.; Mateos, J.; Companyó, X.; Escudero-Casao, M.; Dell'Amico, L. A Rational Approach to Organo-Photocatalysis: Novel Designs and Structure-Property Relationships. *Angew. Chem., Int. Ed.* **2021**, *60*, 1082−1097. (c) Mateos, J.; Rigodanza, F.; Vega-Peñaloza, A.; Sartorel, A.; Natali, M.; Bortolato, T.; Pelosi, G.; Companyó, X.; Bonchio, M.; Dell'Amico, L. Naphthochromenones: Organic Bimodal Photocatalysts Engaging in Both Oxidative and Reductive Quenching Processes. *Angew. Chem., Int. Ed.* **2020**, *59*, 1302−1312.

(6) (a) Bartolomei, B.; Gentile, G.; Rosso, C.; Filippini, G.; Prato, M. Turning the Light on Phenols: New Opportunities in Organic Synthesis. *Chem. - Eur. J.* **2021**, *27*, 16062−16070. (b) Schmalzbauer, M.; Marcon, M.; König, B. Excited State Anions in Organic Transformations. *Angew. Chem., Int. Ed.* **2021**, *60*, 6270−6292.

(7) (a) Balzani, V.; Ceroni, P.; Juris, A. *Photochemistry and Photophysics: Concepts, Research, Applications*; Wiley: 2014. (b) Filippini, G.; Nappi, M.; Melchiorre, P. Photochemical Direct Perfluoroalkylation of Phenols. *Tetrahedron* **2015**, *71*, 4535−4542.

(8) (a) Kobayashi, S.; Higashimura, H. Oxidative Polymerization of Phenols Revisited. *Prog. Polym. Sci.* **2003**, *28*, 1015−1048. (b) Zhang, C.; Xue, J.; Yang, X.; Ke, Y.; Ou, R.; Wang, Y.; Madbouly, S. A.; Wang, Q. From Plant Phenols to Novel Bio-Based Polymers. *Prog. Polym. Sci.* **2022**, *125*, 101473. (c) Guo, Q.; Wang, M.; Liu, H.; Wang, R.; Xu, Z. Visible-Light-Promoted Dearomative Fluoroalkylation of *β*-

Naphthols through Intermolecular Charge Transfer. *Angew. Chem., Int. Ed.* **2018**, *57*, 4747−4751.
(9) (a) Zhu, E.; Liu, X. X.; Wang, A. J.; Mao, T.; Zhao, L.; Zhang, X.; He, C. Y. Visible Light Promoted Fluoroalkylation of Alkenes and Alkynes Using 2-Bromophenol as a Catalyst. *Chem. Commun.* **2019**, *55*, 12259−12262. (b) Schmalzbauer, M.; Ghosh, I.; König, B. Utilising Excited State Organic Anions for Photoredox Catalysis: Activation of (Hetero)Aryl Chlorides by Visible Light-Absorbing 9-Anthrolate Anions. *Faraday Discuss.* **2019**, *215*, 364−378. (c) Liang, K.; Liu, Q.; Shen, L.; Li, X.; Wei, D.; Zheng, L.; Xia, C. Intermolecular Oxyarylation of Olefins with Aryl Halides and TEMPOH Catalyzed by the Phenolate Anion under Visible Light. *Chem. Sci.* **2020**, *11*, 6996−7002. (d) Schmalzbauer, M.; Svejstrup, T. D.; Fricke, F.; Brandt, P.; Johansson, M. J.; Bergonzini, G.; König, B. Redox-Neutral Photocatalytic C−H Carboxylation of Arenes and Styrenes with CO2. *Chem.* **2020**, *6*, 2658−2672.
(10) (a) Nguyen, J. D.; Tucker, J. W.; Konieczynska, M. D.; Stephenson, C. R. J. Intermolecular Atom Transfer Radical Addition to Olefins Mediated by Oxidative Quenching of Photoredox Catalysts. *J. Am. Chem. Soc.* **2011**, *133*, 4160−4163. (b) Wallentin, C.; Nguyen, J. D.; Finkbeiner, P.; Stephenson, C. R. J. Visible Light-Mediated Atom Transfer Radical Addition via Oxidative and Reductive Quenching of Photocatalysts. *J. Am. Chem. Soc.* **2012**, *134*, 8875−8884. (c) Arceo, E.; Montroni, E.; Melchiorre, P. Photo-Organocatalysis of Atom-Transfer Radical Additions to Alkenes. *Angew. Chem., Int. Ed.* **2014**, *53*, 12064−12068. (d) Bag, D.; Kour, H.; Sawant, S. D. Photo-Induced 1,2-Carbohalofunctionalization of C-C Multiple Bonds: Via ATRA Pathway. *Org. Biomol. Chem.* **2020**, *18*, 8278−8293.
(11) Klikar, M.; Solanke, P.; Tydlitát, J.; Bureš, F. Alphabet-Inspired Design of (Hetero)Aromatic Push−Pull Chromophores. *Chem. Rec.* **2016**, *16*, 1886−1905.
(12) The CT excited state of PC **7e** was corroborated by the observed Stokes shift (up to 147 nm) when the emission was measured in PhMe and DMSO. In addition, DFT calculations at M06-2x/Def2TZVP/IEFPCM(CH_3CN) level of theory indicated that for PC **7e** the LUMO is localized on the sulfone moiety, while the HOMO is localized on the phenolate aromatic system (see the Supporting Information).
(13) Altwicker, E. R. The Chemistry of Stable Phenoxy Radicals. *Chem. Rev.* **1967**, *67*, 475−531.
(14) (a) Crisenza, G. E. M.; Mazzarella, D.; Melchiorre, P. Synthetic Methods Driven by the Photoactivity of Electron Donor-Acceptor Complexes. *J. Am. Chem. Soc.* **2020**, *142*, 5461−5476. (b) Arceo, E.; Jurberg, I. D.; Álvarez-Fernández, A.; Melchiorre, P. Photochemical Activity of a Key Donor-Acceptor Complex Can Drive Stereoselective Catalytic α-Alkylation of Aldehydes. *Nat. Chem.* **2013**, *5*, 750−756. (c) Lima, C. G. S.; Lima, T. D. M.; Duarte, M.; Jurberg, I. D.; Paixão, M. W. Organic Synthesis Enabled by Light-Irradiation of EDA Complexes: Theoretical Background and Synthetic Applications. *ACS Catal.* **2016**, *6*, 1389−1407.
(15) (a) Rosso, C.; Williams, J. D.; Filippini, G.; Prato, M.; Kappe, C. O. Visible-Light-Mediated Iodoperfluoroalkylation of Alkenes in Flow and Its Application to the Synthesis of a Key Fulvestrant Intermediate. *Org. Lett.* **2019**, *21*, 5341−5345. (b) Rosso, C.; Filippini, G.; Prato, M. Use of Nitrogen-Doped Carbon Nanodots for the Photocatalytic Fluoroalkylation of Organic Compounds. *Chem. - Eur. J.* **2019**, *25*, 16032−16036. (c) Li, T.; Liang, K.; Tang, J.; Ding, Y.; Tong, X.; Xia, C. A Photoexcited Halogen-Bonded EDA Complex of the Thiophenolate Anion with Iodobenzene for C(Sp^3)−H Activation and Thiolation. *Chem. Sci.* **2021**, *12*, 15655−15661. (d) Bahamonde, A.; Melchiorre, P. Mechanism of the Stereoselective α-Alkylation of Aldehydes Driven by the Photochemical Activity of Enamines. *J. Am. Chem. Soc.* **2016**, *138*, 8019−8030.
(16) Filippini, G.; Silvi, M.; Melchiorre, P. Enantioselective Formal α-Methylation and α-Benzylation of Aldehydes by Means of Photo-Organocatalysis. *Angew. Chem., Int. Ed.* **2017**, *56*, 4447−4451.
(17) (a) Juliá, F.; Constantin, T.; Leonori, D. Applications of Halogen-Atom Transfer (XAT) for the Generation of Carbon Radicals in Synthetic Photochemistry and Photocatalysis. *Chem. Rev.* **2022**, *122*, 2292−2352. (b) Constantin, T.; Zanini, M.; Regni, A.; Sheikh, N. S.; Juliá, F.; Leonori, D. Aminoalkyl Radicals as Halogen-Atom Transfer Agents for Activation of Alkyl and Aryl Halides. *Science* **2020**, *367*, 1021−1026.
(18) (a) Buzzetti, L.; Crisenza, G. E. M.; Melchiorre, P. Mechanistic Studies in Photocatalysis. *Angew. Chem., Int. Ed.* **2019**, *58*, 3730−3747. (b) Cismesia, M. A.; Yoon, T. P. Characterizing Chain Processes in Visible Light Photoredox Catalysis. *Chem. Sci.* **2015**, *6*, 5426−5434.
(19) Corbin, D. A.; Miyake, G. M. Photoinduced Organocatalyzed Atom Transfer Radical Polymerization (O-ATRP): Precision Polymer Synthesis Using Organic Photoredox Catalysis. *Chem. Rev.* **2022**, *122*, 1830−1874.
(20) (a) Plutschack, M. B.; Pieber, B.; Gilmore, K.; Seeberger, P. H. The Hitchhiker's Guide to Flow Chemistry. *Chem. Rev.* **2017**, *117*, 11796−11893. (b) Cambié, D.; Bottecchia, C.; Straathof, N. J. W.; Hessel, V.; Noël, T. Applications of Continuous-Flow Photochemistry in Organic Synthesis, Material Science, and Water Treatment. *Chem. Rev.* **2016**, *116*, 10276−10341. (c) Williams, J. D.; Kappe, C. O. Recent Advances toward Sustainable Flow Photochemistry. *Curr. Opin. Green Sustain. Chem.* **2020**, *25*, 100351. (d) Su, Y.; Straathof, N. J. W.; Hessel, V.; Noël, T. Photochemical Transformations Accelerated in Continuous-Flow Reactors: Basic Concepts and Applications. *Chem. - Eur. J.* **2014**, *20*, 10562−10589.

https://doi.org/10.1021/acscatal.2c00565
ACS Catal. 2022, 12, 4290−4295